Hydrothermal treatment and strontium ion sorption properties of fibrous cerium(IV) hydrogenphosphate

Hiromichi Hayashi,[*a] **Kazuo Torii**[a] **and Shin-ichi Nakata**[b]

[a]*Tohoku National Industrial Research Institute, Nigatake 4-2-1, Miyagino-ku, Sendai 983, Japan*
[b]*R&D Center, Chiyoda Corp., 13 Moriya-cho, Kanagawa-ku, Yokohama 221, Japan*

Fibrous cerium hydrogenphosphate, CeP, has been treated hydrothermally in 1 mol dm^{-3} phosphoric acid solution. CEP and its hydrothermally treated product, CeP(HT), have been characterized by X-ray powder diffractometry, scanning electron microscopy, solid-state ^{31}P MAS NMR spectroscopy, FTIR spectroscopy, chemical and thermal analyses. A poorly crystalline fibrous CeP with a *d*-spacing of 1.1 nm converted into a highly crystalline CeP(HT) with platelet morphology by hydrothermal treatment. Solid-state ^{31}P MAS NMR and FTIR measurements confirmed that one kind of phosphate (H_2PO_4) is present in CeP and two kinds of phosphate (HPO_4, PO_4) are present in CeP(HT), in which the integrated intensity ratio of HPO_4 to PO_4 is 2:1. From chemical and thermal analyses, structural formulae for CeP and CeP(HT) are assumed to be $CeO(H_2PO_4)_2 \cdot 2H_2O$ and $Ce(HPO_4)(PO_4)_{0.5}(OH)_{0.5}$, respectively. The Na^+ exchange capacity of CeP amounted to 4.5 mmol g^{-1} at pH 11 while that of CeP(HT) was less than 1.0 mmol g^{-1} in the pH range 2–12. The pH dependence of the metal ion distribution coefficients exhibited ideal ion-exchange behaviour on CeP while metal ion distribution coefficients on CeP(HT) scarcely depended on pH. The metal ion selectivities of CeP and CeP(HT) increased in the order: $Na^+ < Ca^{2+} < Sr^{2+} < K^+$, and $Na^+ < K^+ < Ca^{2+} < Sr^{2+}$, respectively. The distribution coefficient for the Sr^{2+} ion of CeP(HT) was higher than that of CeP under hydrothermal conditions.

The advent of nuclear technology initiated a search for ion-exchange materials that would be more stable to high temperature and radiation fields than organics. Hence, inorganic ion exchangers are bright prospects for applications in nuclear technology. In many cases, however, synthetic inorganic ion exchangers are amorphous powders or fine crystals, so that they must be granulated with some kind of binder for practical use. Among the various synthetic inorganic ion exchangers, cerium(IV) hydrogenphosphate was the first prepared fibrous ion exchanger, and it can be employed to prepare inorganic ion-exchange papers or thin layers without a binder.[1–3] However, cerium(IV) phosphates constitute a complicated system of compounds.[3–7] The composition is strongly dependent on the preparation conditions, such as temperature and PO_4/Ce molar ratio in solution. Alberti *et al.* obtained four different products: (1) amorphous cerium phosphate with $PO_4/Ce = 1.7$, (2) a microcrystalline cerium phosphate with $PO_4/Ce = 1.15$, (3) another microcrystalline product with $PO_4/Ce = 1.55$ and (4) a fibrous crystalline solid of idealized formula $Ce(HPO_4)_2 \cdot H_2O$.[3] The structure of fibrous cerium hydrogenphosphate has not yet been elucidated owing to its low degree of crystallinity.

In the nuclear reprocessing cycle, the safe disposal of ^{90}Sr activity has always been considered a problem, owing to its long half-life, high thermal neutron fission product and hazardous reactions.[8–10] Fibrous cerium hydrogenphosphate would be applicable to the disposal of ^{90}Sr in radioactive wastes owing to its strong affinity for the Sr^{2+} ion.[2] Despite hydrothermal stability being required for a radioactive Sr^{2+} ion exchanger, few studies have been carried out on exchange properties under hydrothermal conditions.[11] In this regard, hydrothermal stability is anticipated to be endowed by hydrothermal pretreatment of the exchanger. In the present study, fibrous cerium hydrogenphosphate was treated hydrothermally in phosphoric acid solution with variation of temperature and time. The objectives of this study are (1) to characterize the fibrous cerium hydrogenphosphate and its hydrothermally treated product using ^{31}P MAS NMR spectroscopy as well as XRD, SEM, FTIR, chemical and thermal analyses to obtain structural information for both materials, and (2) to demonstrate the effectiveness of both exchangers for Sr^{2+} ion uptake under hydrothermal conditions.

Experimental

Materials

Cerium(IV) sulfate and phosphoric acid [as 85% m/v (*ca.* 17.2 mol dm^{-3}) solution] were GPR grade reagents (Nacalai tesque).

Preparation of cerium hydrogenphosphate

Cerium(IV) hydrogenphosphate (CeP) was prepared as reported by Alberti *et al.*[3] Cerium(IV) sulfate solution (500 cm^3; 0.05 mol dm^{-3}) containing 0.5 mol dm^{-3} sulfuric acid was added dropwise to an aqueous phosphoric acid solution (500 cm^3; 2.4 mol dm^{-3}) with stirring at 90 °C. After 16 h, the yellow solid was filtered off, washed with doubly distilled water and dried at 60 °C.

Hydrothermal treatment of CeP

The resulting cerium(IV) hydrogenphosphate (1 g) and 1 mol dm^{-3} phosphoric acid solution (200 cm^3; 1 mol dm^{-3}) were transferred into a PTFE-lined pressure bottle and subjected to hydrothermal treatment at a constant temperature ranging from 100 to 175 °C for 24, 72 and 168 h. The product was filtered off, washed with doubly distilled water, followed by air-drying at 60 °C.

Physical measurements

X-Ray powder diffraction (XRD) patterns were recorded on a Rigaku Roterflex RU-300 RAD diffractometer using Cu-Kα radiation (35 kV and 50 mA) and a scan speed of 4° min^{-1} in 2θ. The divergent and scattering slits were set at 0.5°, and the receiving slit was 0.3°. Scanning electron microscopy (SEM) studies were carried out with a Hitachi S-800 electron microscope, operating at 15 kV. The ^{31}P MAS NMR spectra were obtained at 109.38 MHz on a Fourier-transform pulsed NMR spectrometer (JEOL JNM-GX270). All ^{31}P NMR spectra combined with magic angle spinning (MAS) at 4.0 kHz were measured with high-power proton decoupling during data acquisition. IR spectra of samples in KBr matrices were measured on a Perkin-Elmer Spectrum 1000 FT IR spectrometer in the range 4000–450 cm^{-1}.

Analysis

Inductively coupled plasma atomic emission spectrometry (KP–AES; Seiko SPS 1200A) was performed for cerium and phosphorus analyses of the samples digested with concentrated hydrochloric acid. Thermogravimetry experiments were carried out on a Rigaku TG-8101D thermogravimetry–differential thermal analyser (TG–DTA) referenced against recalcined alumina. The temperature was ramped at a rate of 10 °C min^{-1} in air.

Ion-exchange equilibria

A 0.1 g sample of the exchanger was immersed in 10 cm^3 of various solutions prepared by the desired combination of 0.1 mol dm^{-3} NaCl and 0.1 mol dm^{-3} NaOH for 168 h at 25 °C with intermittent shaking. The determination of the Na^+ ion concentration was carried out by the atomic absorption method. Distribution coefficients (K_d) were determined for metal ions (Na^+, K^+, Ca^{2+}) at 25 °C and for Sr^{2+} ions every 25 °C in the temperature range 25–150 °C. The initial metal ion concentration was 1×10^{-4} mol dm^{-3} and the pH was adjusted with 0.1 mol dm^{-3} hydrochloric acid. A 0.05 g sample of the exchanger was immersed in 10 cm^3 of a solution with a given pH in a sealable PTFE tube for 168 h at a constant temperature with intermittent shaking. The pH of the supernatant solution was measured by a TOA HM-60S pH meter equipped with a GS-5015 pH combination electrode. The concentration of metal ions was determined by a Hitachi Z-6000 polarized Zeeman atomic absorption spectrophotometer (Na^+, K^+) or a Seiko SPS 1200A ICP emission spectrometer (Ca^{2+}, Sr^{2+}).

The distribution coefficient, K_d, was calculated from eqn. (1)

$$K_d = (C_1/\mathrm{g})/(C_2/\mathrm{cm}^3) \qquad (1)$$

where C_1 is the amount of sorbed ions per 1 g of the solid, and C_2 is the concentration of ions per 1 cm^3 of aqueous solution.

Results and Discussion

Formation and composition

The conditions of hydrothermal treatment and the results of the analysis of the products are summarized in Table 1. Fibrous cerium hydrogenphosphate, with the composition $CeH_2(PO_4)_2 \cdot 3H_2O$, was used as the starting material. Reaction product 1, which was obtained by hydrothermal treatment at 100 °C for 24 h, had still a P : Ce atomic ratio of 2 : 1 whereas the X-ray diffraction pattern was changed from that of the original fibrous cerium hydrogenphosphate. It may be that the reaction does not reach the equilibrium state at 100 °C in 24 h. Irrespective of the hydrothermal conditions, products 2–12 were equilibrium solid phases with a P : Ce atomic ratio of exactly 1.5 : 1. The expected composition was given as $CeH_{0.5}(PO_4)_{1.5} \cdot 0.5H_2O$. Despite the hydrothermal treatment being performed in 1 mol dm^{-3} phosphoric acid solution, a quarter of the phosphate groups were released from the CeP during the hydrothermal treatment.

X-Ray powder diffractometry

The X-ray powder diffraction patterns of CeP and CeP(HT) were measured by using Ni-filtered Cu-Kα radiation. Fig. 1 shows the XRD patterns of CeP and CeP(HT). The XRD pattern of CeP indicated a poorly crystalline phase with only a few lines, the smallest (1.1 nm) being much more intense than the others. The layered structure of CeP was confirmed by the peak shift upon intercalation of octylamine. The interlayer spacing of the octylamine-intercalated CeP increased to 2.8 nm, indicating that octylamine bilayers are formed between the CeP layers. It can be seen clearly from Fig. 1(b) that CeP(HT) is highly crystalline in contrast to CeP. Characteristic peaks corresponding to higher orders of the spacing of 1.05 nm were observed. The diffraction pattern of CeP(HT) matched almost perfectly with that of microcrystalline cerium phosphate with $PO_4/Ce = 1.55$, which was reported previously by Alberti *et al.*[3] This product was obtained by refluxing any type of tetravalent cerium phosphate in concentrated H_3PO_4 solution. The crystallite size of CeP(HT) is shown in Table 1 together with that of CeP. The size of CeP(HT) was larger than that of CeP. In spite of the crystallinity of the product, the structures of CeP(HT) and CeP are unknown. In the case of CeP(HT), evidence for the absence of layering is based on the unchanged spacing upon intercalation of octylamine.

Scanning electron microscopy

Scanning electron microscopic (SEM) observations were performed to examine the texture change of the fibrous CeP after its hydrothermal treatment in 1 mol dm^{-3} phosphoric acid solution at 175 °C for 72 h. As shown in Fig. 2, the photographs revealed that the morphology was changed markedly after the hydrothermal treatment. The original CeP was observed as the fibrils of diameter 20–50 nm. In contrast, CeP(HT) exhibited polycrystalline aggregates of 2–5 μm thin plates with a distinctly crystalline solid, as expected from the XRD pattern.

^{31}P MAS NMR spectroscopy

^{31}P MAS NMR spectroscopy is a powerful technique for studying the environment of metal phosphates since the chemical shift of the phosphate group is remarkably sensitive to its local environment. The ^{31}P MAS NMR spectra for CeP and CeP(HT) are shown in Fig. 3. In the spectrum of CeP, there is a single resonance at δ −7.2 indicating the presence of only one kind of phosphorus environment in the structure of this compound. In contrast, the ^{31}P MAS NMR spectrum of CeP(HT) showed three different resonances at δ −16.2, −27.8 and −29.7 with an intensity ratio close to 1 : 1 : 1.

Many layered tetravalent metal phosphates have structures similar to those of zirconium monohydrogenphosphate, $Zr(HPO_4)_2$; a monohydrate, α, and dihydrate, γ are known. The α-phase has a layer structure consisting of layers of metal atoms in a plane bridged by phosphate groups above and below the plane of metal atoms, with the P—OH groups pointing between the layers.[12] The ^{31}P MAS NMR spectra of layered zirconium phosphates show only one resonance at δ −19 for the α-phase and two resonances of equal integrated intensity at δ −9 and −27 for the γ-phase. The resonance at δ −19 was attributed to the monohydrogenphosphate, $(ZrO)_3POH$. The resonance at δ −27 was assigned to phosphorus atoms of PO_4 tetrahedra.[13] Clayden suggested that substitution of zirconium by hydrogen in the local phosphate group coordinate decreases the bond strength of the oxygens of the phosphate groups, causing a downfield shift in the ^{31}P chemical shift of *ca.* 10 ppm. Thus the signal for γ-zirconium phosphates, δ −9, was assigned as corresponding to $P(OZr)_2(OH)_2$. Accordingly, γ-zirconium phosphate can now be formulated more correctly as $Zr(PO_4) \cdot (H_2PO_4) \cdot 2H_2O$. A layer structure has been proposed for the γ-phase based on the increased spacing of the d_{002} reflection in the X-ray diffraction pattern upon ion exchange; the layers are made up of two ideal planes containing the metal atoms bridged by PO_4 groups in which the dihydrogenphosphate moieties point towards the interlayer region.[14]

Table 1 Hydrothermal treatment and analysis of cerium hydrogenphosphate

	treatment conditions						X-ray analysis	
no.	$T/°C$	t/h	CeO_2 (%)	P_2O_5 (%)	H_2O (%)	product P/Ce (atomic ratio)	d/nm	D/nm^a
1	100	24	39.8	34.5	25.7	2.00	1.11	66
2	100	72	54.8	33.9	11.3	1.50	1.05	204
3	100	168	53.7	33.0	13.3	1.49	1.06	204
4	125	24	54.2	33.5	12.3	1.50	1.06	204
5	125	72	53.5	33.7	12.8	1.53	1.07	295
6	125	168	53.7	33.2	13.1	1.50	1.05	231
7	150	24	53.6	33.2	13.2	1.50	1.05	241
8	150	72	53.0	33.3	13.7	1.52	1.05	241
9	150	168	53.3	33.6	13.1	1.52	1.06	253
10	175	24	53.0	33.1	13.9	1.51	1.05	253
11	175	72	53.7	33.2	13.1	1.50	1.06	312
12	175	168	57.8	35.2	7.0	1.48	1.04	200
starting material			43.2	36.2	20.6	2.01	1.13	10

^{a}Crystallite size calculated using the Scherrer equation.

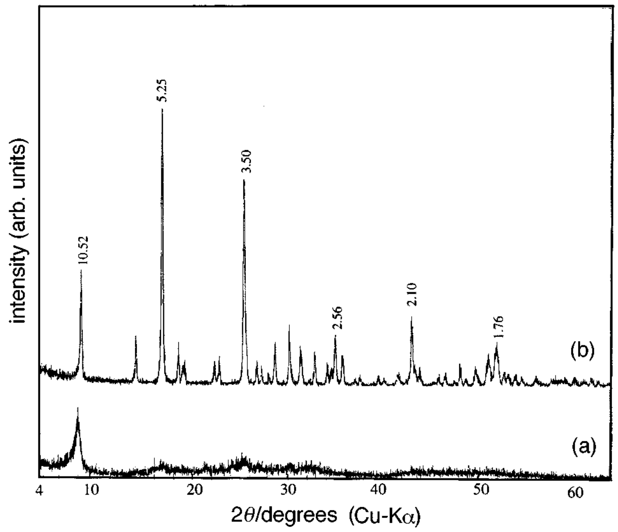

Fig. 1 X-Ray powder diffraction patterns for the fibrous cerium hydrogenphosphate (a) and its hydrothermally treated product (b)

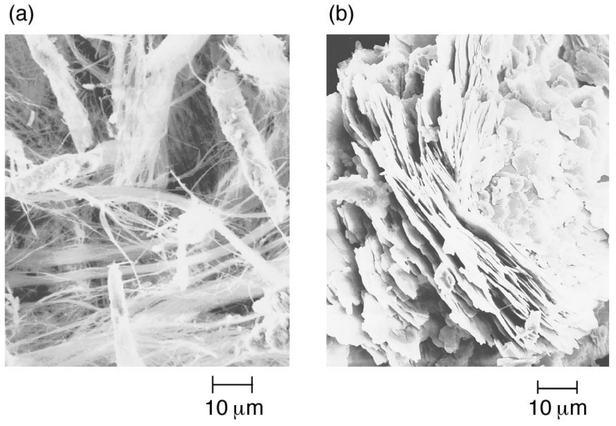

Fig. 2 Scanning electron micrographs illustrating the fibrous texture of the original cerium hydrogenphosphate (a) and the platelet texture of its hydrothermally treated product (b)

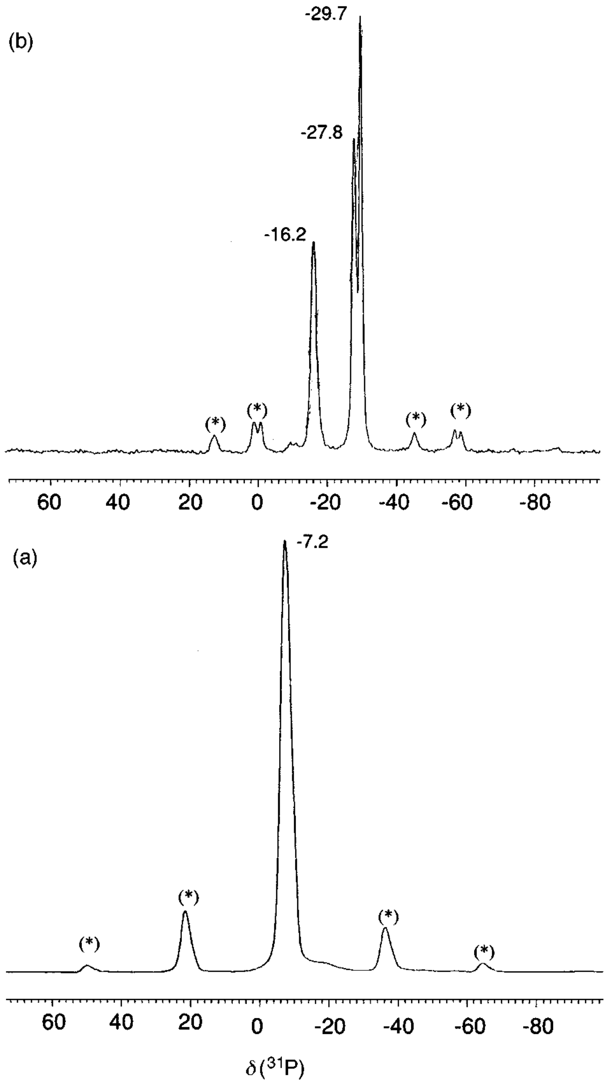

Fig. 3 Solid-state ^{31}P MAS NMR spectra for the fibrous cerium hydrogen phosphate (a) and its hydrothermally treated product (b). Peaks marked with an asterisk are spinning sidebands.

In the present spectra, only one resonance is seen at δ -7.2 for CeP, indicating that one kind of phosphorus environment is present, as in α-zirconium phosphate, whereas the chemical shift is close to δ -9 as observed in γ-zirconium phosphates rather than δ -19 in α-zirconium phosphate. Thus the resonance at δ -7.2 can be assigned as corresponding to $P(OCe)_2(OH)_2$. The ^{31}P MAS NMR spectrum of CeP(HT) gave three resonances at δ -16.2, -27.8 and -29.7. The first resonance can be assigned to $P(OCe)_3(OH)$. The resonances at δ -27.8 and -29.7 are very similar to the ^{31}P resonances in $HZr_2(PO_4)_3$ where the ^{31}P chemical shifts are δ -28.4 and -29.4.[15] The resonance at δ -27.8 can be ascribed to phosphorus atoms of PO_4 tetrahedra.[16] The other resonance at δ

-29.7 corresponds to POH terminal groups as well as the resonance at δ -16.[17] This is supported by the fact that two kinds of resonance at δ -27 and -29 are observed in heat-treated γ-zirconium phosphate where the resonance at δ -29 was enhanced as a function of the cross-polarization time between the ^{1}H and ^{31}P spin systems corresponding to the protonic characteristics of POH group.[18] The ratio of integrated intensities at δ -16.2, -27.8 and -29.7 was 1:1:1. Therefore, the structural formula for CeP(HT) can be postulated to be $Ce(HPO_4)(PO_4)_{0.5}(OH)_{0.5}$.

IR spectra

The ^{31}P MAS NMR results were supported by IR spectroscopy. The IR spectra of the original CeP and CeP(HT) are shown in Fig. 4. The spectrum of CeP shows few bands in the region of 4000–450 cm^{-1}; the broad bands with absorption maxima at 3402 and 1632 cm^{-1} were assigned to the O—H stretching and bending vibrations of interlayer water. The bands at 1150–1000 cm^{-1} represent PO_3 vibrations. The original fibrous CeP showed a broad absorption band at 1061 cm^{-1} due to ν(P—O).[18] In contrast, in the spectrum of CeP(HT), the band in the region of 1200–900 cm^{-1} split to give bands at 1233, 1094, 1035 and 944 cm^{-1}, which revealed that several kinds of phosphate groups exist. The band at 1233 cm^{-1} indicates the presence of monohydrogenphosphate groups.[7] The band at 944 cm^{-1} can be attributed to the bending mode of P—O—P. The bands at 3534 and 1611 cm^{-1} were attributed to the O—H stretching and bending modes of structural water.

Structural formulae for CeP and CeP(HT)

From the chemical and thermal analyses as well as ^{31}P MAS NMR and FTIR results, the structural formulae for CeP and CeP(HT) were postulated as $CeO(H_2PO_4)_2 \cdot 2H_2O$ and $Ce(HPO_4)(PO_4)_{0.5}(OH)_{0.5}$. $CeO(H_2PO_4)_2 \cdot 2H_2O$ requires: CeO_2, 44.5; P_2O_5, 36.9; H_2O, 18.6% and $Ce(HPO_4)(PO_4)_{0.5}(OH)_{0.5}$ requires: CeO_2, 54.1; P_2O_5, 33.5; H_2O, 12.4%. The agreement between the calculated and experimental values was good.

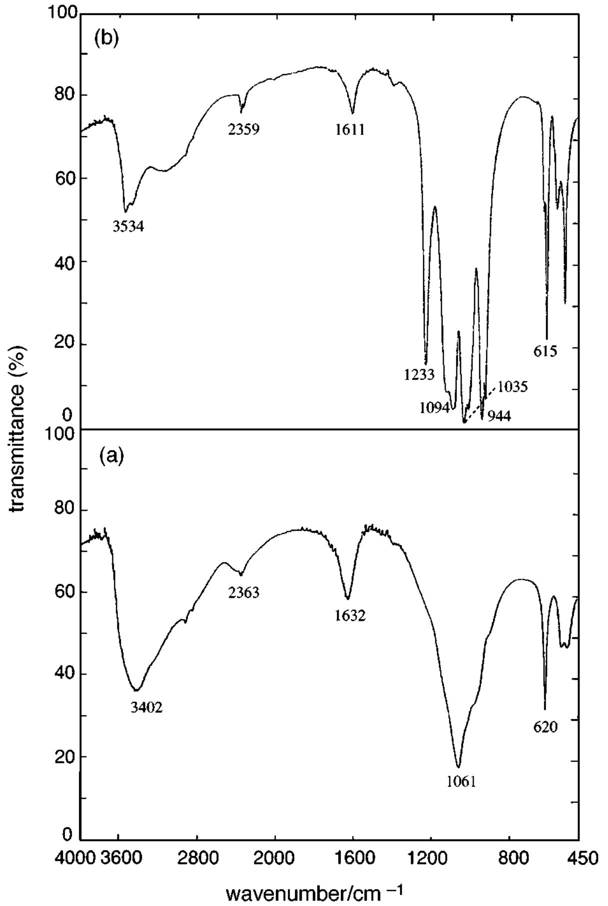

Fig. 4 FTIR spectra for the fibrous cerium hydrogenphosphate (a) and its hydrothermally treated product (b)

Alberti *et al.* pointed out the possible formula for CeP; $CeO(H_2PO_4)_2$ from thermal analyses.[3] The structural formula for CeP(HT) was compatible with $Ce(HPO_4)_{1.1}(PO_4)_{0.45}(OH)_{0.45} \cdot 0.33H_2O$ that was proposed by Herman and Clearfield.[7]

Na exchange capacity

Fig. 5 shows the Na^+ uptake of CeP and CeP(HT), respectively. In the case of CeP, the uptake increased linearly with pH indicating a monofunctional exchange site for the phosphate groups. The titration curve of CeP does not have distinct plateaux, as in the case of layered materials, but a sloping curve is usually obtained as in the amorphous inorganic ion exchangers. From the Na^+ uptake curve of fibrous CeP an experimental ion-exchange capacity of 4.6 mequiv. g^{-1} is obtained at pH 11. The CeP had an exchange capacity close to half of the expected value (10.4 mequiv. g^{-1}) based upon the assumption that protons of the dihydrogenphosphate groups are exchangeable. Only one hydrogen of each dihydrogenphosphate group would be exchanged at pH 11. The second dissociation of dihydrogenphosphate should be difficult owing to the electrostatic attraction by the negative charges of the phosphate groups. Thus, only half of the hydrogen ions were exchanged with Na^+ ions in the pH range 1–11 on the pH titration curve.

The titration curve for CeP(HT) shows that this material does not exhibit appreciable exchange in the pH range 1–12. In the wide pH range Na^+ uptakes are less than 1 mequiv. g^{-1}, which is less than theoretical exchange capacity of CeP(HT) (1.7 mequiv. g^{-1}). As expected from XRD results, CeP(HT) does not possess a layered structure; it seems to have a smaller pore size and thus exhibits a screening effect for ions that diffuse without difficulty in the CeP.

Distribution coefficient

In order to examine the selectivities of CeP and CeP(HT) for metal ions, distribution coefficients, K_d, were measured as a function of pH. Measurements were carried out with some

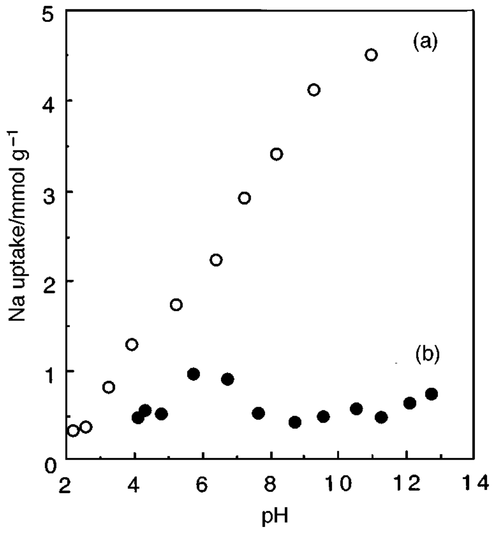

Fig. 5 Na^+ uptakes of (a) the fibrous cerium hydrogenphosphate and (b) its hydrothermally treated product as a function of pH. Exchanger 0.1 g; initial concentration of Na^+ ions 0.1 mol dm^{-3}; vol. 10 cm^3; *T* 25 °C.

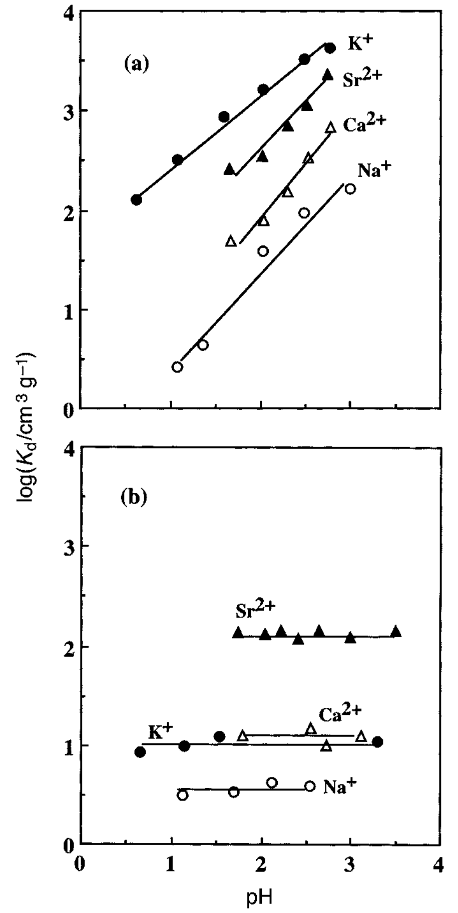

Fig. 6 Distribution coefficients for metal ions (Na^+, K^+, Ca^{2+}, Sr^{2+}) of the fibrous cerium hydrogenphosphate (a) and its hydrothermally treated product (b) as a function of pH. Exchanger 0.05 g; initial concentration of metal ions 1.0×10^{-4} mol dm^{-3}; vol. 10 cm^3; *T* 25 °C.

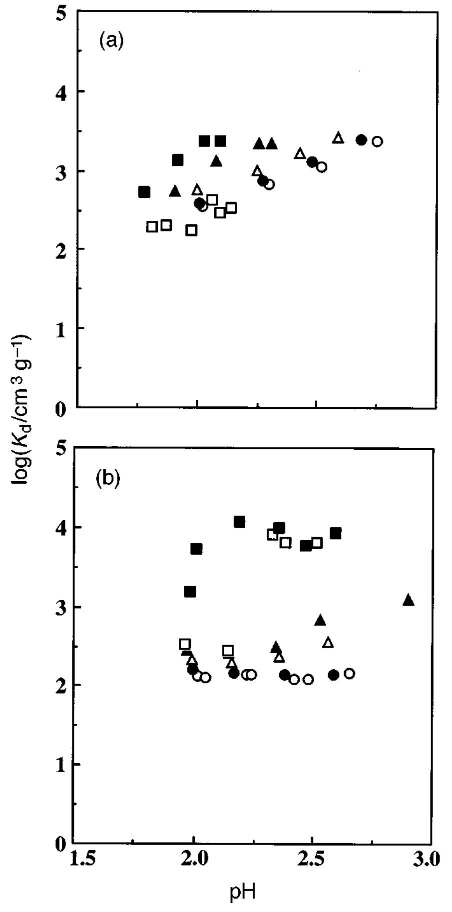

Fig. 7 Distribution coefficients for Sr^{2+} ion of the fibrous cerium hydrogenphosphate (a) and its hydrothermally treated product (b) as a function of pH. Exchanger 0.05 g; initial concentration of metal ions 1.0×10^{-4} mol dm^{-3}; vol. 10 cm^3; *T*: ○, 25; ●, 50; △, 75; ▲, 100; □, 125; ■, 150 °C.

alkali-metal (Na^+ and K^+) and some alkaline-earth-metal (Ca^{2+} and Sr^{2+}) ions. Fig. 6(a) gives the plots of log K_d *vs.* pH for Na^+, K^+, Ca^{2+}, Sr^{2+} ions on CeP. The results show that the selectivity exhibited by CeP increases in the sequence $Na^+ < Ca^{2+} < Sr^{2+} < K^+$. The slopes of the plots for Na^+ and K^+ ions are approximately unity and those for Ca^{2+} and Sr^{2+} are two, indicating that ideality for ion-exchange reaction between metal ions and hydrogen ions can be expected to hold for CeP.

Plots of K_d *vs.* pH for CeP(HT) are shown in Fig. 6(b). Strangely, K_d values scarcely depend on the pH. The reason for this exchange behaviour is not clear, but may be attributed to the fact that only surface sites are available for the exchange reaction due to the screening effect mentioned above. It was observed that the K_d value increases in the sequence $Na^+ < K^+ < Ca^{2+} < Sr^{2+}$. CeP(HT) exhibits an unexpected selectivity for Sr^{2+} whereas the K_d values for each of the metal ions were lower than those of CeP.

Temperature dependence of Sr^{2+} uptake

The temperature dependence of the distribution coefficients for Sr^{2+} ions on CeP and CeP(HT) as a function of pH is shown in Fig. 7. In the case of CeP, plots of K_d *vs.* pH shifted to lower pH as the temperature was increased to 100 °C, suggesting that ion exchange between Sr^{2+} ions and H^+ ions is an endothermic reaction.[19] Above 100 °C, although the K_d value decreased slightly at 125 °C, it increased subsequently at 150 °C to retain the sorption ability under hydrothermal conditions. The dissociation constant increased with the temperature owing to the decreasing dissociation constant of water.[20] The second dissociation of dihydrogenphosphate groups provides suitable sites for divalent metal ions. In the case of CeP(HT), K_d values were enhanced markedly at 100 °C or higher, whereas the K_d values were lower than those of the CeP below 100 °C. Dehydration of Sr^{2+} ions and acceleration of the dissociation of hydrogenphosphate groups seem to be the reasons for the enhanced Sr^{2+} sorption activity on CeP(HT) under hydrothermal conditions. Powder X-ray diffraction patterns of the products after reacting in Sr^{2+} solution at 150 °C were determined. The XRD pattern of CeP(HT) was unchanged after the reaction suggesting that it is hydrothermally stable, while fibrous CeP was collapsed at 100 °C or higher.

Conclusions

Hydrothermal treatment of fibrous cerium hydrogenphosphate leads to the condensation of phosphate groups; subsequently the layers are firmly cross-linked to give a non-expandable structure. The condensation of phosphate groups affects the selectivity for metal ions as well as the ion-exchange capacity. Under hydrothermal conditions, Sr^{2+} sorption behaviour on the hydrothermally treated product is more useful than that of the original cerium hydrogenphosphate owing to the hydrothermal stability in addition to the selectivity for Sr^{2+} ion. Since Sr^{2+} uptake can be achieved by cerium hydrogenphosphate and its hydrothermal product under hydrothermal conditions, both materials are of great promise as an adsorbent for ^{90}Sr. Further studies are being conducted to elucidate the Sr^{2+} sorption mechanism under hydrothermal conditions.

References

1 G. A. Alberti, M. A. Massucci and E. Torracca, *J. Chromatogr.*, 1967, **30**, 579.
2 G. A. Alberti, M. Casciola, U. Costantino and M. L. Luciani, *J. Chromatogr.*, 1976, **128**, 289.
3 G. A. Alberti, U. Costantino, F. Di Gregorio, P. Galli and E. Torracca, *J. Inorg. Nucl. Chem.*, 1968, **30**, 295.
4 G. A. Alberti, U. Costantino and L. Zsinka, *J. Inorg. Nucl. Chem.*, 1972, **34**, 3549.
5 K. H. Konig and E. Meyn, *J. Inorg. Nucl. Chem.*, 1967, **29**, 1153.
6 E. M. Larsen and W. A. Cilley, *J. Inorg. Nucl. Chem.*, 1968, **30**, 287.
7 R. G. Herman and A. Clearfield, *J. Inorg. Nucl. Chem.*, 1975, **37**, 1697.
8 T. Sasaki, Y. Komatsu and Y. Fujiki, *Chem. Lett.*, 1981, 957.
9 N. Yamasaki, K. Yanagisawa, S. Kanahara, M. Nishioka, K. Matsuoka and J. Yamazaki, *J. Nucl. Sci. Technol.*, 1984, **21**, 71.
10 D. K. Bhattacharyya and N. C. Dutta, *J. Mater. Sci.*, 1995, **30**, 2248.
11 S. Ahrland and G. Carleson, *J. Inorg. Nucl. Chem.*, 1977, **33**, 2229.
12 A. Clearfield and G. D. Smith, *Inorg. Chem.*, 1969, **8**, 431.
13 N. J. Clayden, *J. Chem. Soc., Dalton Trans.*, 1987, 1877.
14 A. N. Christensen, E. K. Andersen, I. G. K. Andersen, G. Alberti, M. Nielsen and M. S. Lehmann, *Acta Chem. Scand.*, 1990, **44**, 865.
15 N. J. Clayden, *Solid State Ionics*, 1987, **24**, 117.
16 K. Nakashiro, Y. Ono, S. Nakata and Y. Morimura, *Zeolites*, 1993, 561.
17 L. Maistriau, Z. Gabelica, E. G. Derouane, E. T. C. Vogt and J. van Oene, *Zeolites*, 1991, 583.
18 K. Segawa, S. Nakata and S. Asaoka, *Mater. Chem. Phys.*, 1987, **17**, 181.
19 H. Hayashi, T. Iwasaki, T. Nagase, Y. Onodera and K. Torii, *Solvent Extr. Ion Exch.*, 1995, **13**, 1145.
20 F. H. Sweeton, R. E. Mesmer and C. F. Baes, Jr, *J. Solution Chem.*, 1974, **3**, 191.

Paper 6/06397G; *Received* 17*th September*, 1996